Vietnam Journal of Earth Sciences, 44(1), 33-54, https://doi.org/10.15625/2615-9783/16594

Vietnam Academy of Science and Technology
Vietnam Journal of Earth Sciences
http://www.vjs.ac.vn/index.php/jse

Evaluation of the Global Satellite Mapping of Precipitation (GSMaP) data on sub-daily rainfall patterns in Vietnam

Thanh-Hoa Pham-Thi[1*], Jun Matsumoto[1,2], Masato I. Nodzu[1]

[1]*Department of Geography, Tokyo Metropolitan University, Minami-Osawa, Hachioji, Tokyo192-0397, Japan*
[2]*Department of Coupled-Ocean-Atmosphere-Land Processes Research, Japan Agency for Marine Earth Science and Technology, Yokosuka, Kanagawa 237-0061, Japan*

Received 28 May 2021; Received in revised form 29 August 2021; Accepted 29 September 2021

ABSTRACT

This study aims to evaluate the performance of Global Satellite Mapping of Precipitation (GSMaP) data in observing the sub-daily rainfall patterns in Vietnam using synoptic gauge measurements considering seasonal variations in rainfall. Differences in the estimations of the three GSMaP products, including the standard version 7 (MVKv7) and two gauge-calibrated versions 6 and 7 (GAUv6 and GAUv7), were clarified based on rainfall characteristic parameters and statistical indices. The present study clarified that the contribution of sub-daily rainfall in Vietnam was higher during the afternoon than at other times, predominantly in the Central Highlands and Southern Plain, while it occurred most often during the evening to early morning in northern regions. Distinct regional features were also identified along the central coast. Most of the summer afternoon maximum fell in the western mountainous area, while the eastern coastal plain experienced an insignificant amount of rainfall. As rainfall characteristics varied with seasons and regions, the performance of GSMaP demonstrated this variation quite well compared to in-situ observations. However, GSMaP still exhibited high biases in rainy season and topographically heterogeneous areas, especially in the northern regions where sub-daily rainfall cycles had large variations. The standard GSMaP (MVK) product illustrated an afternoon peak better than the gauge-calibrated (GAU) product, which suggests that utilizing the MVK in the Central Highlands and Southern Plain and the GAU over central coastal regions would be appropriate when considering the characteristics of sub-daily precipitation.

Keywords: GSMaP, Sub-daily rainfall, Seasonal variation, Vietnam.

1. Introduction

Climate generally reflects the responses of aquatic, terrestrial, and atmospheric systems to solar forcing over a defined time during which seasonal and diurnal variations are considered to be fundamental (Xiao et al., 2018). With the development of remote sensing techniques, the daily and sub-daily scales have been received increasing attention because excessive amounts of rainfall in a

*Corresponding author, Email: hoa.phamthithanh.vn@gmail.com

short period can cause inundation and flash floods that severely affect human life and environment. Under global warming scenarios, scientific data on the variation of rainfall intensity, frequency, and duration are required urgently to thoroughly understand the underlying processes (Lewis et al., 2019).

As a component of the sub-daily scale, diurnal variations intensify notably during pre-summer or summertime conditions but present less weakly during other seasons (Oki and Musiake, 1994; Li et al., 2008; Chen et al., 2009; Watters and Battaglia, 2019; Battaglia et al., 2019). In terms of the spatial distribution of rainfall, peaks are usually observed at midnight or in the early morning at coastal regions and downstream plains, both of which are associated with large-scale circulations and offshore breezes (Oki and Musiake, 1994; Carbone et al., 2002; He and Zhang, 2010; Yuan et al., 2012; Chen et al., 2018; Minobe et al., 2020). In contrast, the frequency of inland rainfall is at its maximum from the afternoon to early evening and is associated mainly with terrain or the destabilization of the boundary layer due to solar heating (Dai, 2001b; Ohsawa et al., 2001; Yu et al., 2007). In terms of contributions to daily levels, Ohsawa et al. (2001) and Takahashi et al. (2010) both found that a higher portion of rainfall occurred in the early morning instead of the frequent afternoon rainfall that occurred over inland areas of tropical Asia. This contrasted with the findings of Hirose and Nakamura (2005) and Chen (2020), who showed that diurnal rainfall was more dominant over the Indochina Peninsula or in southeastern China during afternoon hours.

Vietnam, which has a coastline of approximately 3,260 km excluding islands, is within a tropical region, but its climate is diverse along its length. The summer rainy season generally begins in early May in most regions (Matsumoto, 1997; Wang and LinHo, 2002; Nguyen-Le et al., 2014, 2015). However, in the central coastal area, the rainy season occurs later in autumn to early winter when the activities of tropical cyclones and northeasterly winds mainly involved (Yokoi and Matsumoto, 2008; Nguyen-Le and Matsumoto, 2016). While there are four distinct seasons (spring, summer, fall, and winter) in northern Vietnam, there is only a difference between dry and rainy seasons in the southern regions. The characteristics of sub-daily rainfall in the tropical Asian region, including Vietnam, showed significant differences in terms of the time at which they peaked and their underlying climatic processes. However, most research related to sub-daily patterns or diurnal rainfall has paid more attention to summers when convective activities are evident (Ohsawa et al., 2001; Hirose and Nakamura, 2005; Takahashi et al., 2010).

Despite the controversial approaches used to identify sub-daily rainfall, in-situ datasets have proved to have outstanding reliability, particularly over rural regions or areas of complex terrain. This is because in-situ data are directly measured compared to remotely sensed products, including satellite-based rainfall estimates with a high spatial and temporal resolution. The Tropical Rainfall Measuring Mission (TRMM) satellite, which was launched in 1997 (Kummerow et al., 2000), has successfully provided a baseline for several popular rainfall datasets used in many studies, including those on diurnal rainfall (Nesbitt and Zipser, 2003; Takahashi et al., 2010). More recently, the Japan Aerospace Exploration Agency (JAXA) has developed the Global Satellite Mapping of Precipitation (GSMaP) product as a high-resolution dataset using infrared and multiband passive microwave sensors (Kubota et al., 2009). However, the performance of

GSMaP showed diverging uncertainties over various regions owing to several aspects of the nature of satellite rainfall estimation, including inaccuracies in the measurement of cloud top temperature, thermal radiance, or cloud system structures. According to Ushio et al. (2009), the performance of the standard GSMaP product was comparable to other remotely sensed products, such as the Climate Prediction Center (CPC) morphing method (CMORPH; Joyce et al., 2004) and TRMM 3B42RT (Huffman et al., 2007). Morover, Guo et al. (2015) suggested that the gauge-calibrated GSMaP product was even better (Guo et al., 2015). Although measuring rainfall via satellite has an advantage over rain-gauge measurement in terms of the spatiotemporal resolution of the data obtained, there remain uncertainties regarding the availability of sensors and the fact that precipitation retrieval algorithms are still being evaluated and calibrated to verify rainfall estimates. Regional factors, such as interactions between topography and low-level winds, have been found to have significant influences on these estimates (Kubota et al., 2007; Shige et al., 2013; Ngo-Duc et al., 2013; Mega and Shige, 2016). For example, the GSMaP reanalysis version 6 product was comparable with in-situ observations in the central coastal regions of Vietnam; however, it produced underestimations in the Central Highlands region (Trinh-Tuan et al., 2019). The GSMaP Microwave-Infrared Combine Reanalysis Product (GSMaP RNL) version 6 produced remarkable regional differences in northern Vietnam, with high positive biases in the coastal regions and negative biases in the mountainous areas (Nodzu et al., 2019). These studies mainly investigated seasonal, monthly, and daily rainfall characteristics estimated by the GSMaP. There has been relatively little work on using GSMaP products to study the sub-daily variation of precipitation.

The energy and water cycles strongly affect variations in convective activities and rainfall in different seasons and regions. Thus, the accuracy of satellite-based precipitation relies on assumptions like precipitation regime, temperature profiles, or cloud characteristics which vary with time, locations, and satellites' sensors. For instance, infrared-based rainfall algorithms often have a time lag between the strongest convective activities and the maximum rainfall, which results from an analysis of diurnal variation of summer convection (Pfeifroth et al., 2016). Understanding the finer intervals of rainfall cycles can provide insights into the microclimate over a particular region, thus contributing to improving physical parameterizations in climate models and understanding the accuracy of remotely sensed precipitation. Therefore, by using a denser rain gauge network with a finer horizontal resolution, this study aims to analyze sub-daily features of rainfall and investigate the capability of GSMaP products to reproduce sub-daily rainfall patterns with regard to seasonal variations by focusing primarily on Vietnam, a country with a diverse climate, where the characteristics of diurnal precipitation cycles have not been studied in detail.

The remainder of this paper is organized as follows. Section 2 outlines the data and methodology used to investigate characteristics of sub-daily rainfall patterns and quantitatively evaluate the performance of GSMaP products. Section 3 presents the features of sub-daily cycles and the seasonal changes using both in-situ gauge and satellite estimations in Vietnam and assesses the accuracy of the three GSMaP products at estimating rainfall. Section 4 discusses the results obtained, and Section 5 summarizes the study and presents its conclusions.

2. Dataset and Methodology

2.1. Rainfall datasets

The GSMaP estimated surface rainfall by combining a passive microwave-infrared algorithm (Joyce et al., 2004) and a Kalman filter that deduced the rate of rainfall regulated by a forward-backward morphing technique from infrared images (Ushio et al., 2009). The gauge-calibrated GSMaP_Gauge (GAU) product was created by optimizing the standard version of the dataset, GSMaP_MVK (MVK), with the widely used gauge-based CPC rainfall dataset (Mega et al., 2019). This study investigated the sub-daily cycle of rainfall in terms of seasonality using in-situ observations and three GSMaP products, namely the MVK version 7 (MVKv7), GAU version 6 (GAUv6), and GAU version 7 (GAUv7), to evaluate and analyze the differences in their performances over Vietnam. The spatial resolution of the three GSMaP products was 0.1° of longitude and latitude. In addition, data from 168 rainfall measurement stations across Vietnam provided by the National Center for Hydro-Meteorological Forecasting (NCHMF), the Vietnam Meteorology and Hydrology Administration (VNMHA) were used to validate the rainfall estimates from the GSMaP. The names and numerical orders of these stations are listed in Pham-Thi and Matsumoto (2021). All precipitation data covered from March 2014 to October 2018. Every six-hourly GSMaP data in a day (including 00–06, 06–12, 12–18, 18–00 UTC) were combined to ensure that the dataset was compatible with in-situ observations that measured the amount of rainfall within the last six hours up to specific synoptic hours (0600, 1200, 1800, and 0000 UTC, respectively). For example, the value measured at 0000 UTC represented the rainfall accumulated from 1800 UTC on the previous day to 0000 UTC. With the "GMT+7" being the local time (LT) zone in Vietnam, the converted hours were 0700, 1300, 1900, and 0100 LT and denoted early morning, afternoon, evening, and midnight in terms of the measurement time, which gives the rainfall occurred in early morning, late morning, afternoon, and late evening, respectively. The terrain information with a spatial resolution of 1 km was obtained from the Global Land One-Kilometer Base Elevation (GLOBE) Project (Hastings and Dunbar, 1999).

The 168 stations mentioned previously, seven climatic subregions of Vietnam, and the maximum number of calibrated stations at each grid at 0.5° of longitude and latitude in the CPC dataset used as part of the GSMaP GAU products during the study period are shown in Fig. 1.

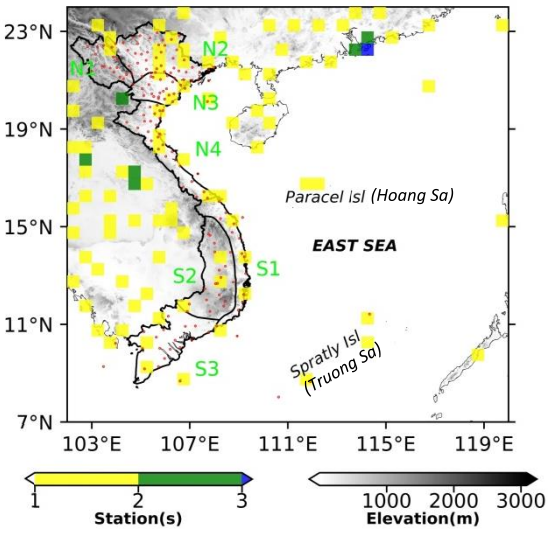

Figure 1. Location of in-situ stations used in this study (red dots) and maximum number of rain gauge-calibrated stations for each 0.5-degree grid of the Climate Prediction Center (CPC) Unified Gauge-Based Analysis of Global Daily Precipitation dataset (colored squares). The topographical map with its gray-scale bar was obtained from the Global Land One-km Base Elevation (GLOBE) dataset. Map of the seven climatic subregions in Vietnam: the Northwest (N1), Northeast (N2), Northern Delta (N3), North Central (N4), South Central (S1), Central Highlands (S2), and Southern Plain (S3)

2.2. Methodologies

Sub-daily rainfall, which was computed at each grid in the satellite dataset and from in-situ station measurements, was characterized by its accumulation, intensity, frequency, and contribution to daily totals. As described above, to be comparable with the synoptic rain-gauge observation, which was measured four times per day (including 0000, 0600, 1200, and 1800 UTC), we produced the 6-hourly GSMaP datasets based on the initially hourly data. Hence, we used the unit of the accumulated precipitation in six hours up to the above four times for both the in-situ observation and the GSMaP throughout this study, with the unit of the rain rate being "mm/6 h".

Accumulation was the mean of the above six-hourly rainfall within the study period, which included both rain and no-rain events and was calculated as follows:

$$AC = \frac{1}{M}\sum_{j=1}^{M} R_j \quad (1)$$

where Rj represents the level of six-hourly accumulated rainfall at measuring times j at each station in the in-situ dataset or each grid in the satellite rainfall product, and M is the number of six-hourly observations.

Intensity was the average of total rainfall events when rainfall levels exceeded 0.1 mm/6h and calculated using the following formula:

$$IN = \frac{1}{K}\sum_{j=1}^{K} R_j^* \quad (2)$$

where R_j^* indicates a level of rainfall greater than 0.1 mm at time j and K is the number of times when the amount of rainfall was greater than 0.1 mm.

Rainfall frequency is defined as the percentage of time rainfall levels were greater than 0.1 mm for all events N and was calculated as below:

$$FR = \frac{K}{N} \times 100 \quad (3)$$

The contribution to the daily total was computed by taking the percentage of the six-hourly rainfall amount that fell between specific time spans to the sum of the rainfall amount at all four-time spans of the study period. This shows the portion of rainfall that fell during a particular time span with respect to the daily accumulated amount:

$$C = \sum_{j=1}^{K} R_j / \sum_{i=1}^{N} R_i \quad (4)$$

Here, Rj represents the amount of rainfall at time step j, including the measurement times (0700, 1300, 1900, and 0100 LT), while Ri represents the amount of rainfall at time step i over observation time N.

The mean error (*ME*) and normalized standard deviation (*STDN*) were the two statistical verification parameters used to validate the performance of GSMaP against the in-situ dataset, as in Pham-Thi and Matsumoto (2021). The formulas are as follows:

$$ME = \frac{1}{N}\sum_{i=1}^{N} (P_i - O_i) \quad (5)$$

$$STDN = \frac{STD\ (P)}{STD\ (O)} \quad (6)$$

Here, Pi is the satellite-measured rainfall level at the grid point nearest the gauge-based station, Oi is the amount of rainfall observed by a gauge at time i, and STD, P, and O are the standard deviation, satellite-measured estimate, and in-situ observation, respectively. The *ME* and *STDN* were calculated for each gauge station.

3. Results

3.1. General patterns of sub-daily rainfall cycles

The characteristics of accumulation, contribution to daily total, intensity, and frequency of the sub-daily rainfall, including the analysis from the in-situ dataset and three GSMaP products, are presented in Figs. 2-5, respectively. The "annual" feature refers to the properties of rainfall regardless of its seasonal variations. All four analyses generally showed a similar rhythm of sub-daily rainfall patterns. They reached an afternoon peak in southern Vietnam (S3 and a

part of S2) and the southern central coastal region (S1), while the maximum accumulation tended to occur in the evening and early morning in northern Vietnam (N1 and N2). The contribution of six-hourly rainfall to daily totals was aligned with the accumulation maxima pattern, with the most considerable portion (approximately 40–80%) and the highest intensities occurring during the afternoon hours in the southern Vietnam region, which is located south of 17°N, as shown in Figs. 3, 4.

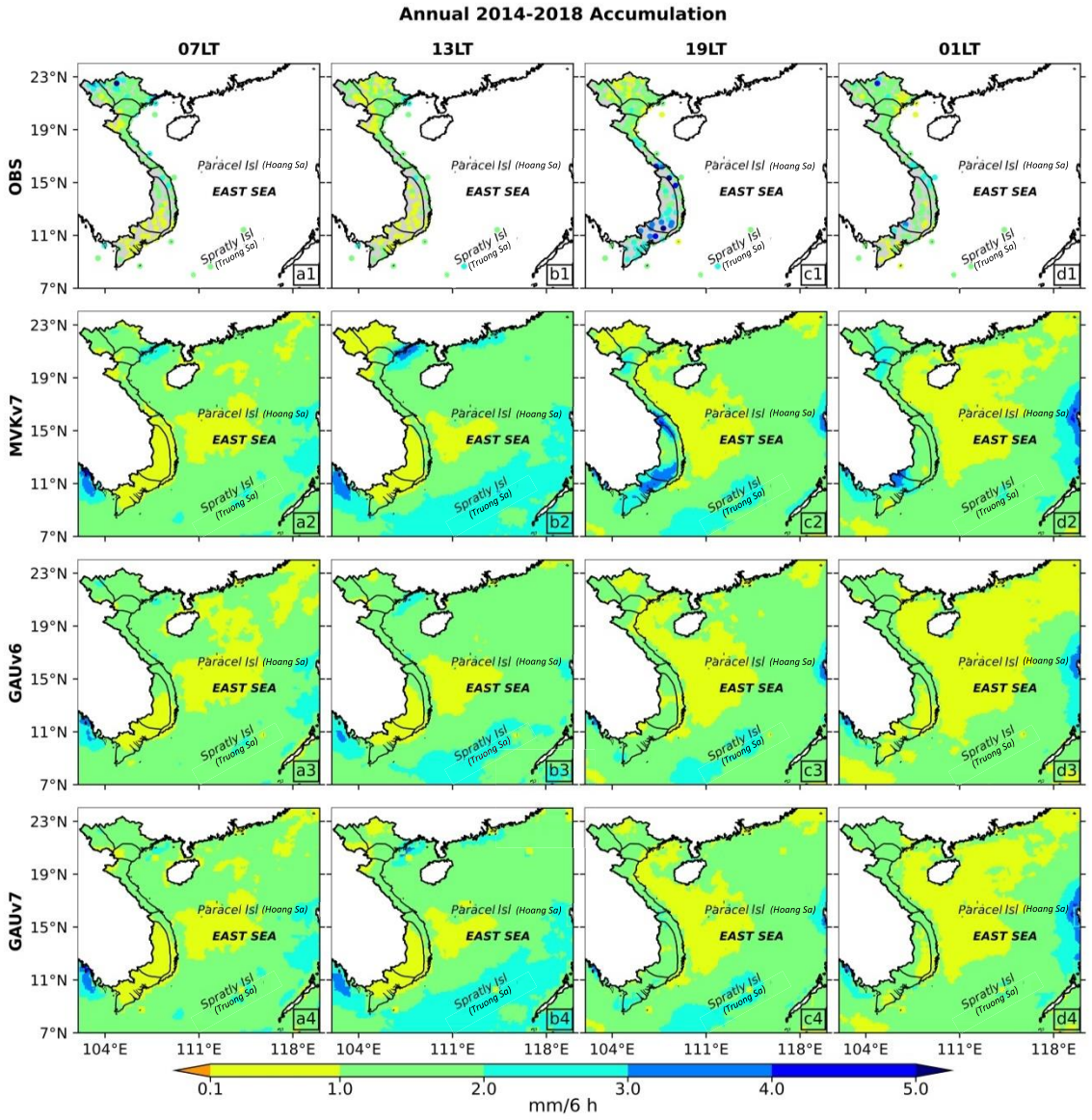

Figure 2. Annual accumulation levels for sub-daily rainfall patterns at 0700, 1300, 1900, and 0100 local time (LT) as computed via gauge observations (OBS), GSMaP Standard version 7 (MVKv7), GSMaP Gauge-calibrated version 6 (GAUv6), and GSMap Gauge-calibrated version 7 (GAUv7). Boundaries of the seven climatic subregions in Vietnam are shown by black lines

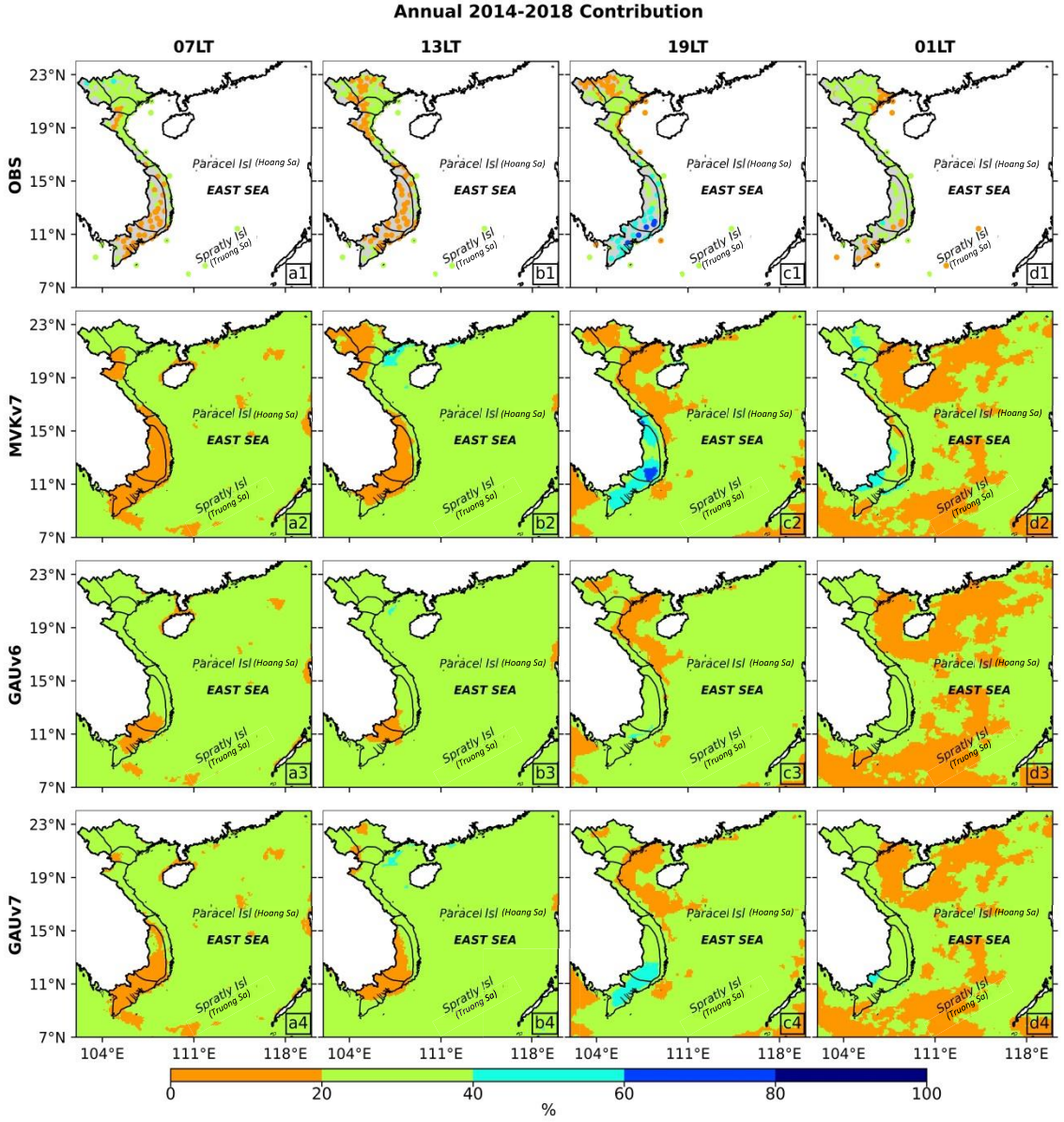

Figure 3. Same as Fig. 2 but for the contribution to daily rainfall

In terms of the estimation of rainfall by the GSMaP products, the results showed that the distribution of the maximum afternoon rainfall was captured well in the results from MVKv7, while the other two GAU products largely underestimated this, although the patterns they reproduced were quite similar to the observations (Fig. 2). In addition, MVKv7 tended to overestimate the accumulated rainfall at 1300 and 0100 LT on the northern coast (N2) and northern delta plain (N3), respectively; these were also the areas where the greatest positive errors were seen in Pham-Thi and Matsumoto (2021) (Fig. S1).

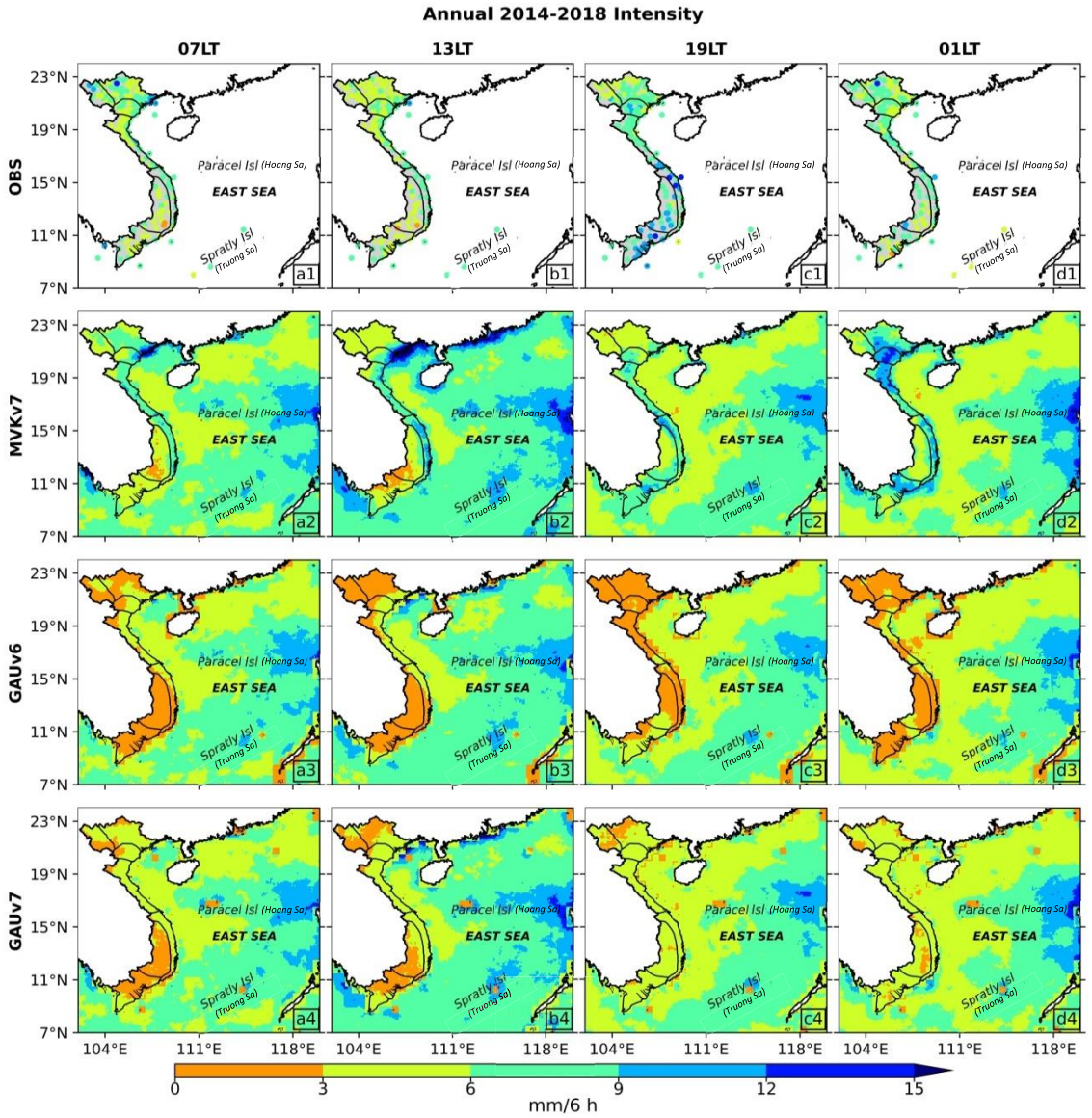

Figure 4. Same as Fig. 2 but for the intensity defined by the average of total rainfall events where rainfall levels exceeded 0.1 mm (6 hours)$^{-1}$

The reason seems to have been the intensification of the quantity of rainfall rather than a change in rainfall frequency because an overestimation in intensity was mostly observed over this region when maps showing the intensity and frequency (Figs. 4, 5) were compared. The differences between GAUv6 and GAUv7 were seen clearly in such analysis, suggesting that the effect of the upgraded gauge calibration method in the newer version was apparent. Despite providing a better estimation for the northern coastal region in the morning, both GAUv6 and GAUv7 seriously underestimated patterns for the afternoon, to an extent worse than that found in MVKv7. Moreover, the "Rain/No-Rain" classification or the detection of light rain in the GSMaP algorithms was

questionable, particularly in the GAU products, as the frequency analysis (Fig. 5) suggested a higher frequency of rainfall levels greater than or equal to 0.1 mm/6 h over the Vietnam region. This was also seen in the work of Pham-Thi and Matsumoto (2021), who found that the GSMaP GAUv7 had a wider bias range than MVKv7 in the six-hourly rainfall threshold levels "<0.15 mm/6 h" and "1.5–4.0 mm/6 h" (Fig. S2). Although the results of the spatial distribution for contribution to the daily total, frequency, and intensity on land in GAUv7 were better than those in GAUv6, the former still performed poorly for island stations, underestimating and overestimating accumulation, respectively, on near-shore islands and offshore islands, particularly the Spratly Islands, during the day.

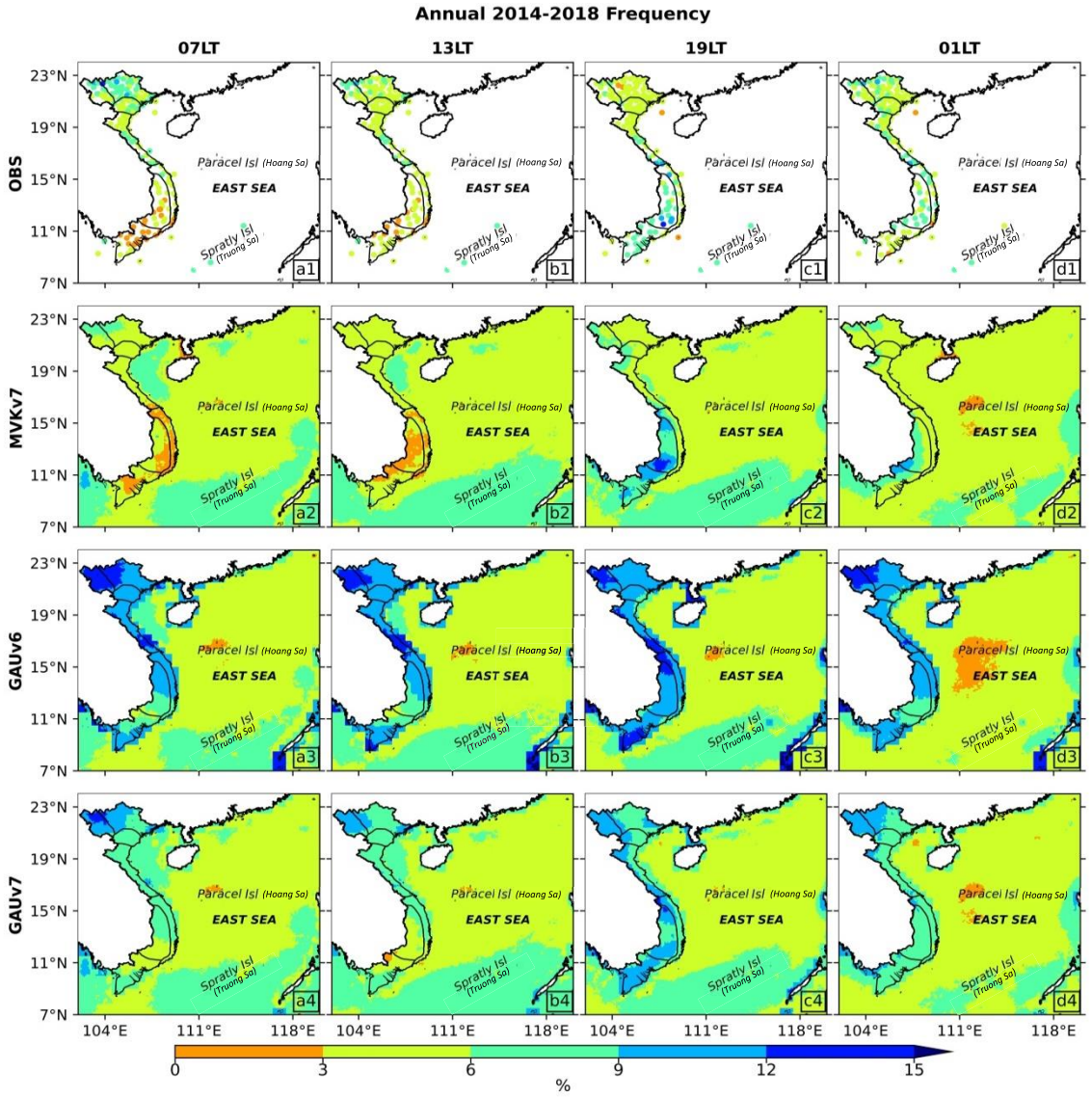

Figure 5. Same as Fig. 2 but for the frequency defined by the ratio of time observing precipitation exceeding 0.1 mm (6 hours)$^{-1}$ to all the observational time

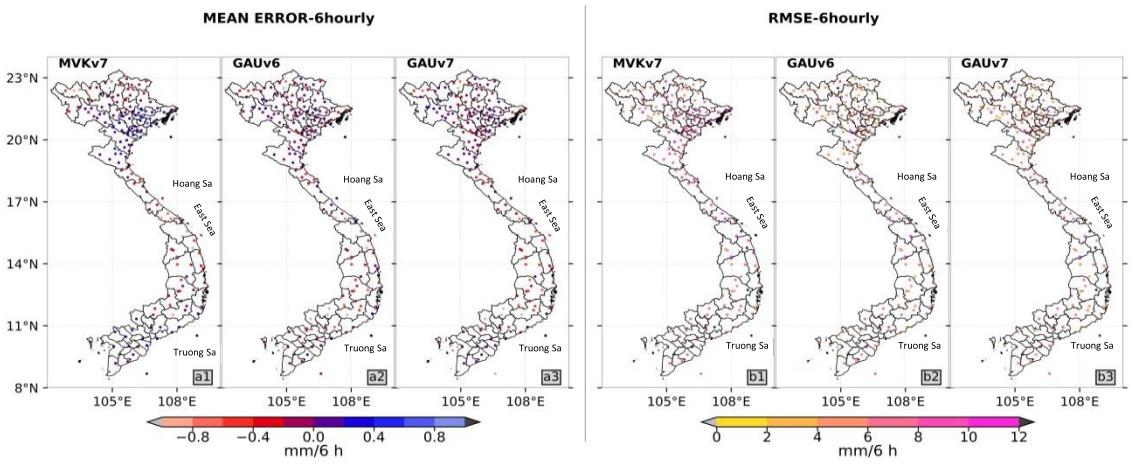

Figure S1. Mean error (a1, a2, and a3) and root mean square error (b1, b2, and b3) of the satellite rainfall estimation (MVKv7, GAUv6, and GAUv7) with the rain gauge dataset (OBS) for the 6-hourly accumulated rainfall (from Pham-Thi and Matsumoto 2021)

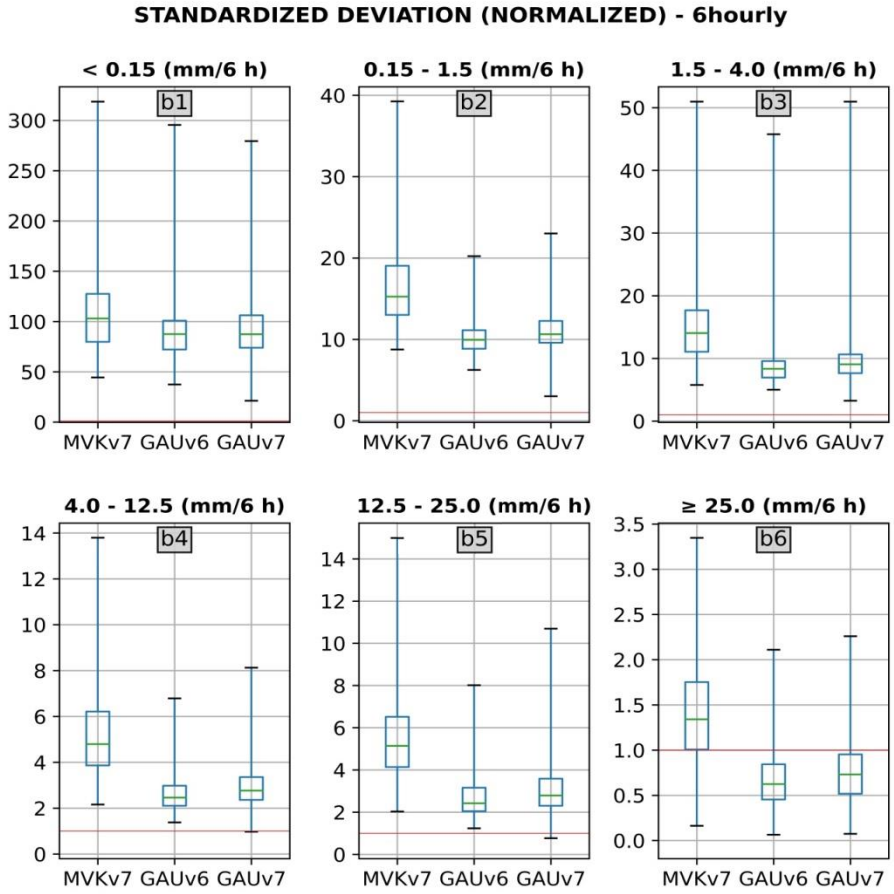

Figure S2. Normalized standard deviation of satellite rainfall estimation data (including MVKv7, GAUv6, and GAUVv7) and the rain gauge dataset of 6-hourly accumulated rainfall (b1, b2, b3, b4, b5, and b6) based on six rainfall thresholds. The red line is the ratio value equal to 1 and corresponds to the best performance of satellite estimation (from Pham-Thi and Matsumoto 2021)

3.2. Seasonal variations in sub-daily rainfall cycles

As previously mentioned, there are regional discrepancies in the rainy season in Vietnam. However, previous studies that investigated the sub-daily or diurnal rainfall characteristics just focused on those in summers, when convective activities are strong (Ohsawa et al., 2001; Hirose and Nakamura, 2005; Takahashi et al., 2010). In this study, the features of the sub-daily cycles of rainfall in Vietnam are analyzed for all seasons. In addition to considering the sub-daily variations, the seasonality is considered based on seasonal changes in precipitation and low-level zonal wind data taken from Nodzu et al. (2019). The year was divided into three periods the January-February-March-April (JFMA), May-June-July-August (MJJA), and September-October-November-December (SOND) seasons.

Although there was less rainfall in the JFMA season than in the others (Fig. 6), the maximum rainfall level in the afternoon was clearly visible in the S2 and S3 regions where the intensity levels also witnessed least varied between three seasons. In contrast, nocturnal and morning precipitation contributed mostly to the rainfall measured in the northern mountainous regions.

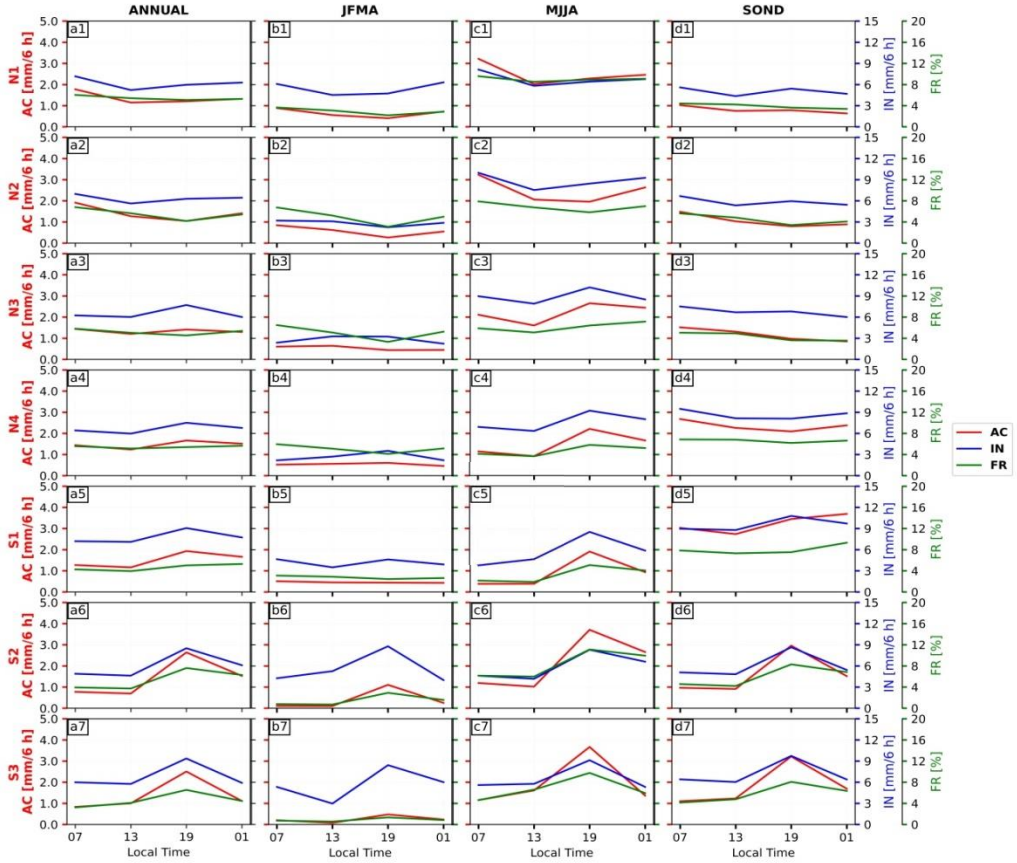

Figure 6. Sub-daily variation of the regional average of accumulation, intensity, frequency in the annual analysis, January-February-March-April, May-June-July-August, and September-October-November-December seasons computed from in-situ observations. The 1st, 2nd, 3rd, 4th, 5th, 6th, and 7th rows illustrate the calculations for regions N1, N2, N3, N4, S1, S2, and S3, respectively. In the figure, the abbreviations AC, IN, and FR, respectively, stand for accumulation, intensity, and frequency

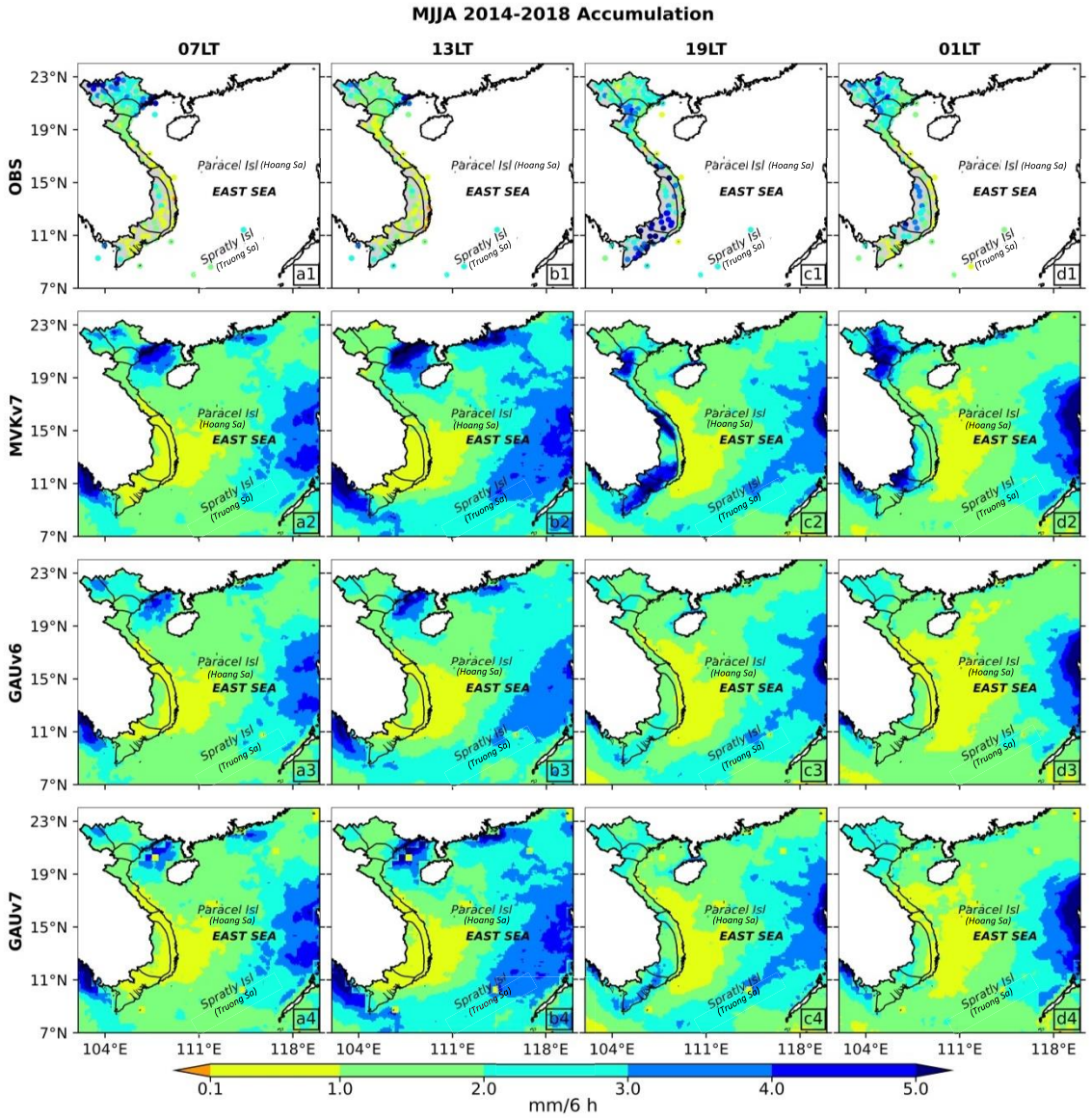

Figure 7. Seasonal sub-daily accumulation levels at 0700, 1300, 1900 and 0100 local time (LT) computed via observations (OBS), GSMaP Standard version 7 (MVKv7), GSMaP Gauge-calibrated version 6 (GAUv6) and GSMaP Gauge-calibrated version 7 (GAUv7) for the May-June-July-August (MJJA) season. Boundaries of the seven climatic subregions in Vietnam are shown by black lines

The rainy season in the central regions (N4 and S1) began when the northeast winter monsoon patterns gradually replaced those of the summer monsoon during the SOND season. The sub-daily cycle of rainfall seemed to appear unclear in SOND, with the levels of accumulated rainfall generally remaining unchanged within a day (Fig. 9). In contrast to the conditions in the MJJA season, GAUv6 and GAUv7 captured the rainfall values of central coastal regions better than MVKv7 during this period for most time intervals; the

exception was the level of rainfall that accumulated at 1900 LT. Bias in rainfall intensity and frequency distribution contributed to the reduction in the performance of the standard product, which will be further analyzed in Section 4. However, it is worth noting that most of the rain gauge-calibrated stations in the CPC dataset were located near the coast and not in the western area in the N4 and S1 regions (Fig. 1a). Additionally, the opposite seasonal variation in precipitation and monsoon winds in the MJJA and SOND seasons differed in western and eastern areas. Thus, the rain gauge-calibrated GAU products became more accurate than the MVK data during SOND.

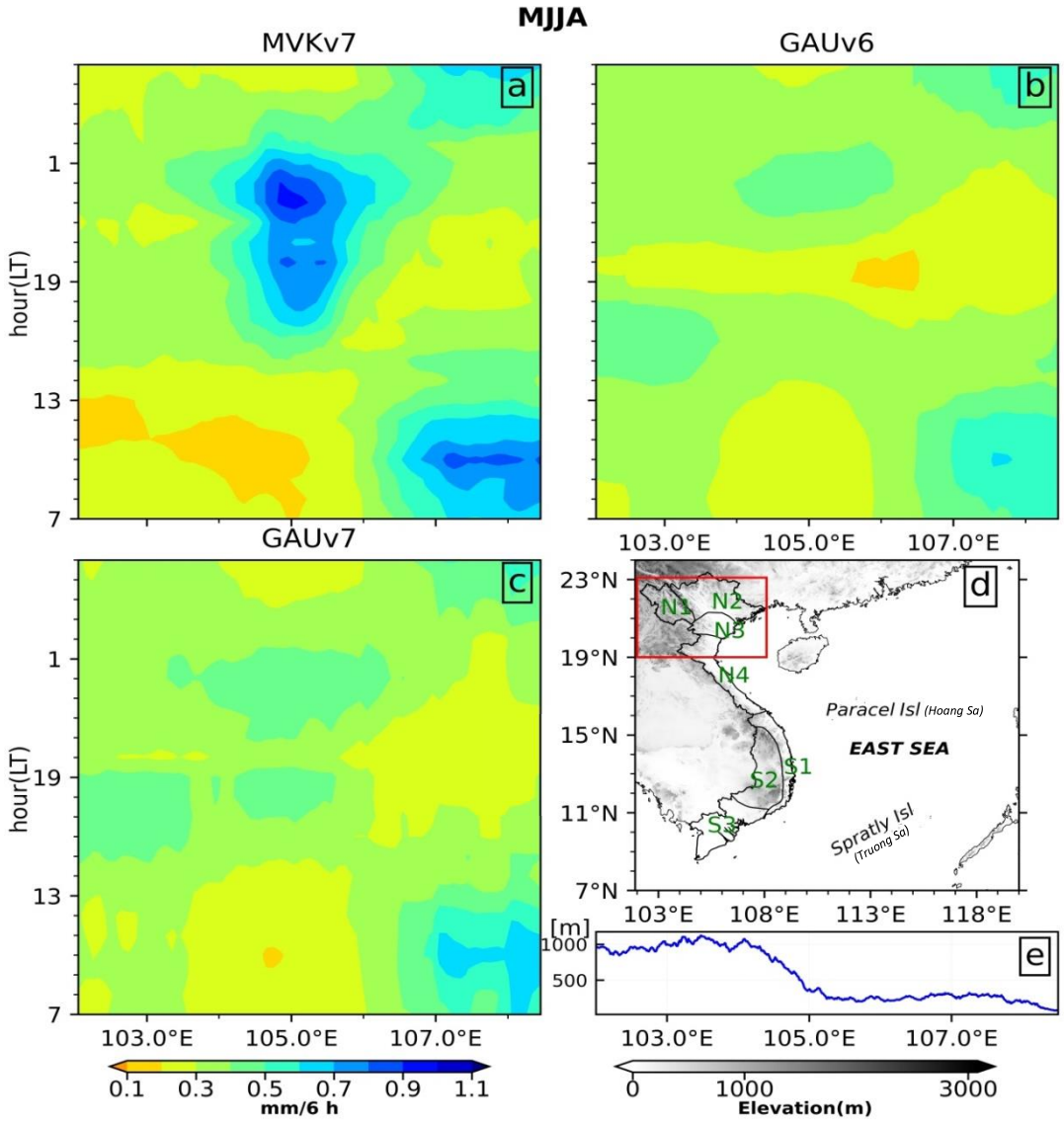

Figure 8. Time-longitude cross-section of hourly rainfall over regions of northern Vietnam (presented in the red rectangle in (d)) estimated by (a) MVKv7, (b) GAUv6, and (c) GAUv7. (e) A topographical cross-section of the area

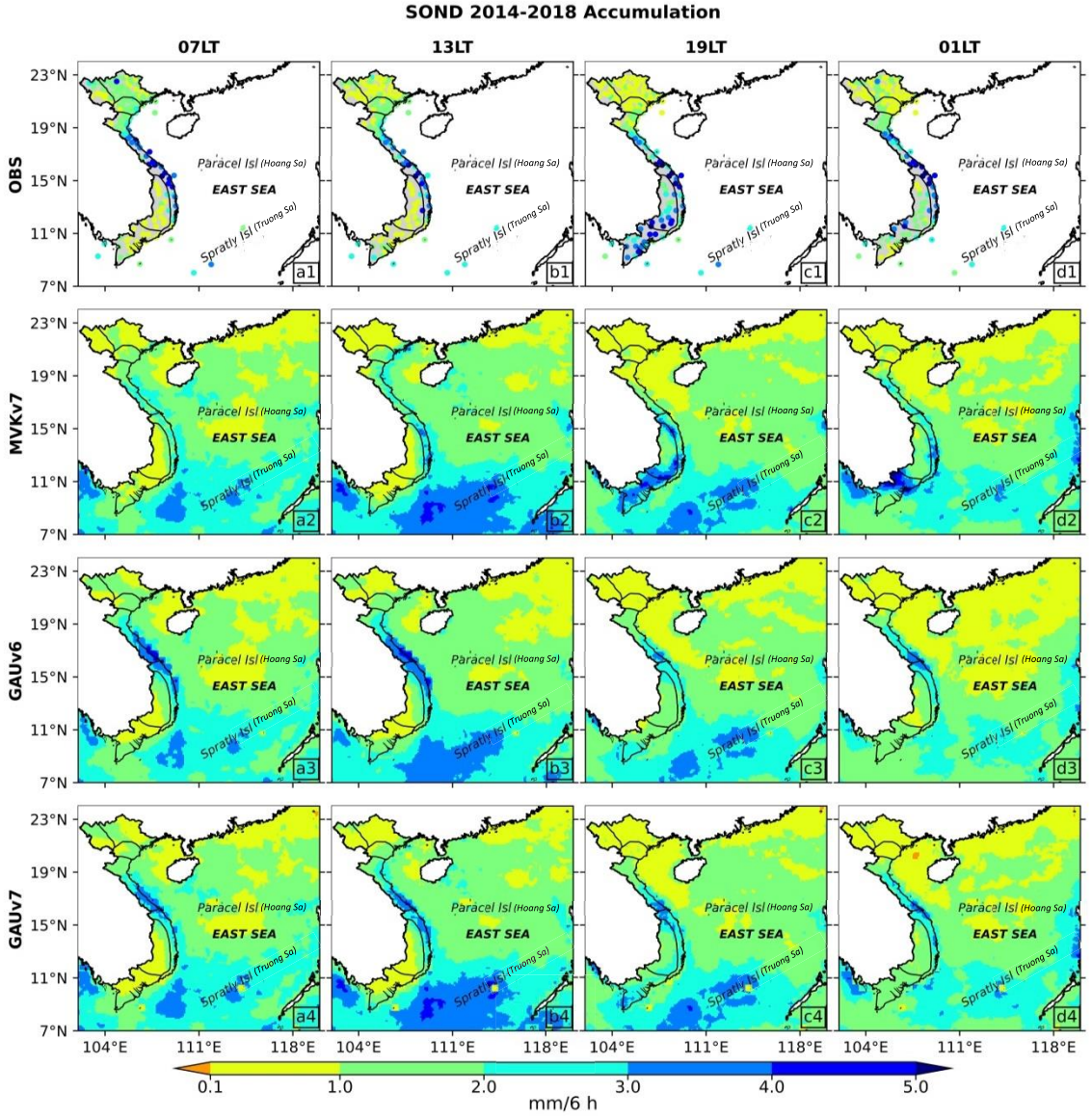

Figure 9. Same as Fig. 7 but for the September-October-November-December (SOND) season

Three GSMaP products showed that the sub-daily variations in rainfall over the Vietnamese East Sea (VES) varied less than those over land and were more significant in the MJJA and SOND seasons. These products performed well the southward movement of rainfall systems over these seasons (Figs.7 and 9, the accumulation of the sub-daily rainfall in JFMA was not shown). The most expansive areas of rainfall and those that experience the most significant rainfall intensity were observed over the VES in the morning of the MJJA season. This is consistent with the findings of Takahashi (2016). In addition, among the three products, GAUv7 often underestimated rainfall on isolated islands, particularly the Spratly Islands-which revealed that the GAU product algorithm that calibrated the grid from a daily dataset on isolated islands was unsuitable for the sub-daily or diurnal analysis.

3.3. Assessment of the performances of GSMaP

Previous subsections analyzed the features of the sub-daily cycle of rainfall over regions of Vietnam and found discrepancies in precipitation levels estimated using in-situ measurements and the three GSMaP products. In this subsection, the performances of these satellite-based products were evaluated to determine their capability to reproduce the sub-daily cycle and the seasonality.

Figures 10–12 illustrate statistical evaluations of the three GSMaP products from the rain gauge-observed dataset for each climatic subregion in Vietnam. For the distribution of the *ME*s of six-hourly accumulated rainfall, as shown in the panel "a" of each figure, biases were greater in months during the rainy seasons in the seven climatic subregions in Vietnam. The reasonable sub-daily rainfall cycle investigated in previous subsections was also evident during these rainy seasons. In addition, lower-altitude stations such as those in N1, N2, N3, and S1 produced *ME*s with larger ranges, proving that the relevant findings were related to the effects of orographic rainfall on the performance of GSMaP.

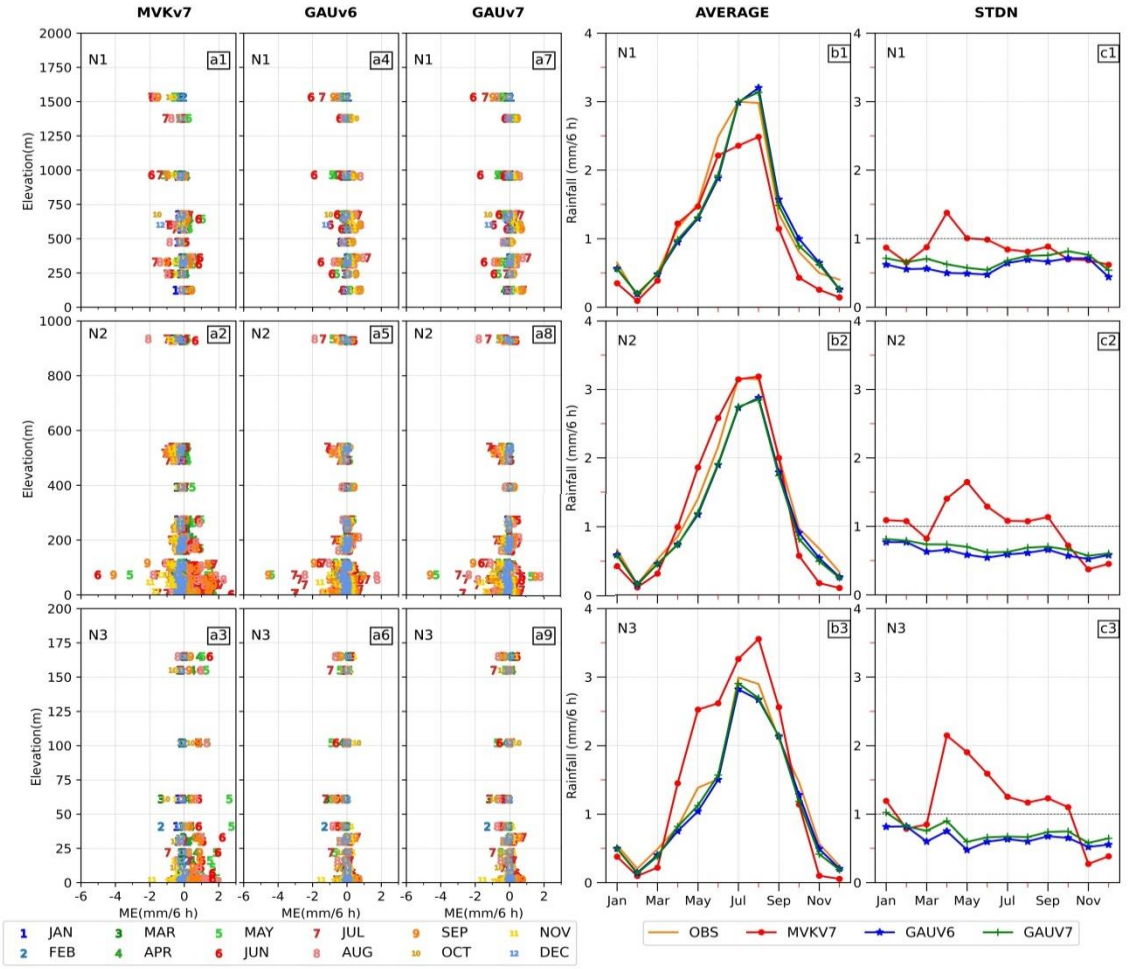

Figure 10. (a1–a9) Scatter plots of mean error and elevation of all stations. (b1–b3) Regional average of six-hourly rainfall by month. (c1–c3) Regional average of normalized standard deviation by month. All figures were created for regions N1, N2, and N3

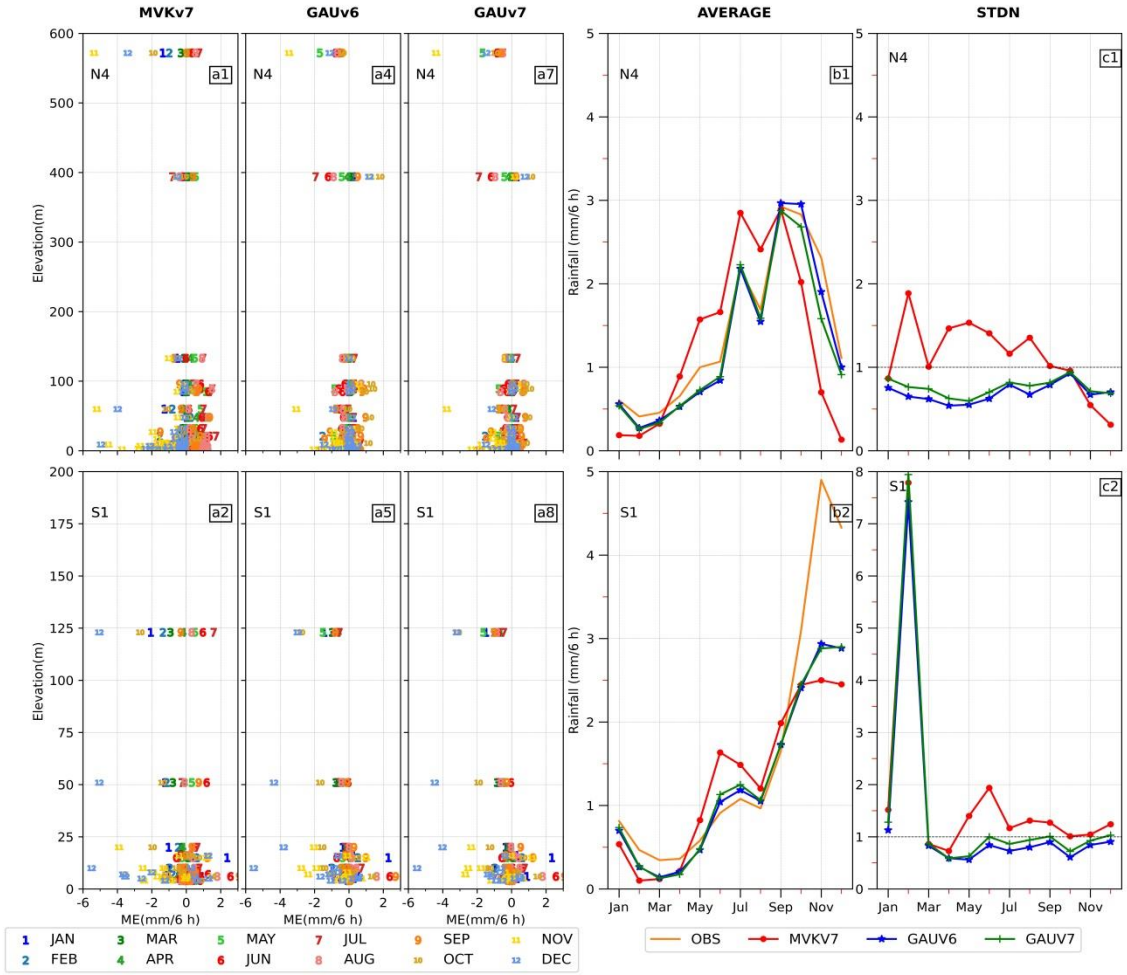

Figure 11. Same as Fig. 10 but for regions N4 and S1

The regionally averaged six-hourly rainfall patterns, as estimated by the three GSMaP products, accorded well with the observational mean. However, the amplitudes of variation in GAUv6 and GAUv7 were lower than the observations, while MVKv7 showed the opposite bias for most regions except the Central Highlands (S2). In northern regions, there were larger errors in transitional months, such as April and September. Meanwhile, remarkable variations were observed in June and from October to December in both the central coastal N4 and S1 regions. Despite the rain-gauge measurement and satellite observations sharing a matching pattern, the MVK performed better than the two GAU products for dry months (i.e., January, April, and November) in the S3 region. For August, the MVK results contrasted with those of GAUv6 and GAUv7 in S2 and S3, i.e., the performance worsened in S2 and improved in S3 (Figs. 12b1 and 12b2). However, the amplitude of the biases seemed to become more complicated when the normalized standard deviation index STDN between GSMaP and observation was accounted for, as this showed that the more the STDN value differed from “1”, the more errors there were in the satellite estimation.

This analysis clearly showed that the efficiency of the GSMaP estimation depended on the climatological season and regional factors such as topography, which are difficult to reproduce using a global calibration algorithm, even such in MVKv7 or GAUv7. Each product demonstrated its superiority in certain areas in a way that favored local features. For example, because most CPC rain gauge stations used in the calibration were located on the coastal plain, the GAU products had an advantage over the MVK product in the S1 region during intense rainy months such as November and December. Meanwhile, MVK had the advantage in estimating rainfall more efficiently in the summer in the S2 and S3 regions, which is consistent with the performance of GSMaP products for the sub-daily precipitation cycle.

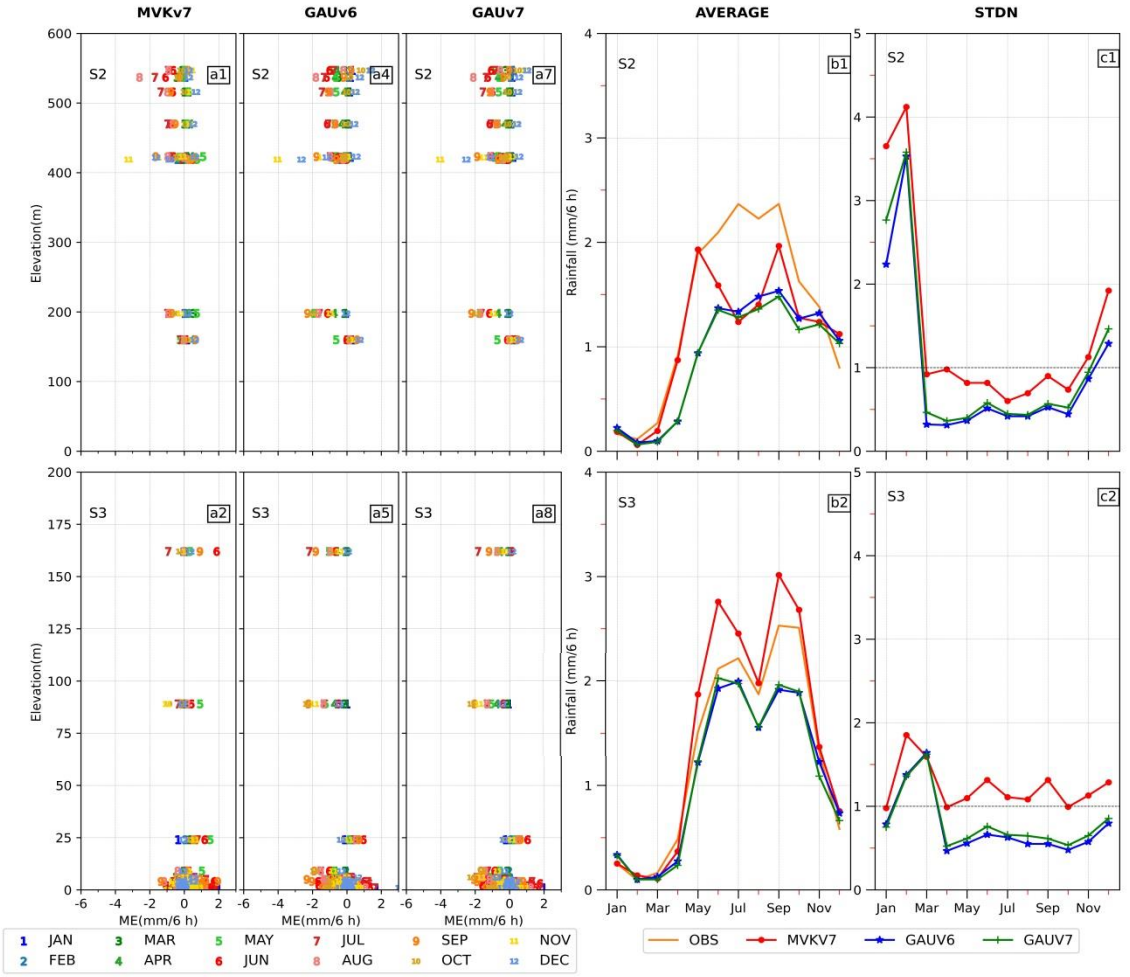

Figure 12. Same as Fig. 10 but for regions S2 and S3

4. Discussions

Early morning rainfall could make a marked contribution to the climatological mean summer rainfall pattern over the Indochina Peninsula (Ohsawa et al., 2001; Takahashi et al., 2010). However, this study showed that the afternoon maximum was more dominant with considerable accumulation and frequency levels in the

southern regions of Vietnam (Fig. 6). This study also showed that there was much regional and seasonal variability in precipitation patterns in the country's northern and central coastal regions. The general sub-daily pattern showed an afternoon to evening peak in the northern deltas (N3), an evening to early morning maximum in the northwestern mountains (N1), and a peak in the early morning to later parts of the morning in the northeastern (particularly coastal) regions. Higher rainfall accumulation levels were measured in the central coastal regions on the western side of the country than in the eastern plains during the MJJA season due to the Foehn phenomenon (Nguyen-Le et al., 2014), as this generated moisture and precipitation on the windward slope and left dry air on the leeward side of the Annam Mountain range. Conversely, the sub-daily features presented less differently in these regions during the SOND seasons, with a high level of rainfall accumulating throughout the day.

Regarding the likely changes in peak phases in northern regions, Bao et al. (2011) found that the propagation of mesoscale convective systems from the eastern edge of the Tibetan Plateau to eastern China was associated with the mountain-plain solenoid circulation. Huang et al. (2010) suggested that this affected the longevity and expansion of convection under prevailing westerly winds. However, Takahashi et al. (2010) analyzed surface winds to show that early afternoon and evening peaks, and even those from the early morning, developed from a different mechanism. This pattern of rainfall cycles in the northern regions appeared in both the MJJA and SOND seasons based on results elaborated on in the previous subsection of this paper. Furthermore, the rainfall accumulation seemed to increase from the afternoon to early morning, although the intensity remained the same. In addition, differences in the results from the three GSMaP products were clearly seen here, with the rainfall levels in MVKv7 being more significant than GAUv6 and GAUv7 (Fig. 8). These require further investigation to analyze and understand the reasons underlying this phenomenon.

Several factors that generate errors in estimates of rainfall for Vietnam made using the GSMaP have been studied previously (Ngo-Duc et al., 2013; Trinh-Tuan et al., 2019; Nodzu et al., 2019). The findings of these studies revealed a great bias caused by the effects of wind and elevation. By investigating the sub-daily cycle associated with seasonal changes, this study found results consistent with the strong dependence of GSMaP on the seasonal and regional features of rainfall, for which there was an extensive error range in the rainy season. Moreover, the quality of the CPC dataset used to calibrate the estimation of the GSMaP GAU products was also important. The distribution of rain gauge-calibrated stations near the coasts enhanced the performance of GAU during the SOND season but reduced it in the MJJA season in the central coastal regions. Furthermore, satellite estimations of rainfall rely mostly on cloud characteristics, but the contributions of the sensor properties and rainfall retrieval algorithms should also be considered. Takahashi (2013) found that diurnal cycles inherent to rainfall are strongly associated with updrafts that resulted in a high cloud top temperature in October, while influxes of cold surges with low-level clouds dominated during winter monsoon months (mostly December and January) in Vietnam. The standard GSMaP products applied a morphing technique from an infrared sensor that might have generated problems due to the influence of warm orographic rain (Dingku et al., 2008; Gao and Liu, 2013). Hence, uncertainties that emerged from the infrared sensor or the algorithm to detect cloud systems could have contributed to the worse

performance of the MVKv7 compared to GAU products during the SOND season in central Vietnam.

5. Conclusions

This study aimed to evaluate the performances of three GSMaP products in reproducing the cycles of sub-daily rainfall in Vietnam and the seasonal changes therein by analyzing statistical indices based on in-situ observations and satellite estimates of rainfall. The results showed the characteristics of sub-daily rainfall and speculations regarding errors in the performances of the three products of GSMaP that are different in calibration methods and versions, thus improved current understanding of the regional differences in the sub-daily rainfall cycle and provided insights on estimating rainfall using remotely sensed data.

The characteristics of the sub-daily rainfall patterns in Vietnam varied by region and season. The most pronounced signal came from the southern regions (including the Central Highlands and the Southern Plain), showing an afternoon peak (13–19 LT) that contributed more than 40% of the daily rainfall. The pattern in the northern regions differed during the summer monsoon period: the northern plain received a large amount of rain mostly during 13–19 LT, while the northwestern mountainous region and the northeastern coast received their peak rainfall during 19–07 LT and 01–13 LT, respectively. The level of rainfall fell significantly in the afternoon of the northern plain from September to December. However, considerable levels of rainfall continued to occur from the night to morning peaks at high frequencies in the northern regions of Vietnam. Sub-daily variation occurred more clearly in summertime over the central regions (N4 and S1) at higher accumulation levels and frequencies over the western side compared to the coastal plains, which was explained by the influence of the Foehn phenomenon in this region. In addition, during the months when there was a northeasterly wind (i.e., the SOND season), there was no significant difference across these regions because the accumulation, frequency, and intensity levels did not vary considerably during six-hourly time spans.

By investigating the sub-daily analysis with seasonal variabilities, the underlying reason for the performance of the GSMaP over Vietnam was determined: as more precipitation accumulated, the GSMaP bias increased. This produced systematic errors during the rainy seasons (MJJA and SOND) across the country. The afternoon peak for the sub-daily cycle was captured more precisely by the MVK product than the GAU product, especially in the Central Highlands and Southern Plain. Thus, the MVK should be used in monitoring the afternoon peaks of rainfall. The GAU product performed better during the fall to the winter season when precipitation characteristics over central coastal regions were accounted for because of the distribution of validation stations near the coast. Nevertheless, the estimation of rainfall using GAUv7 on isolated islands raised questions due to its considerable underestimation in comparison with those in GAUv6. The reason why the GAU algorithm could not well modify the MVK with gauge observation should be studied in the future.

Finally, because the pattern of nocturnal rainfall in the northwestern mountains and rainfall characteristics over the northeastern coast cannot yet be explained by large-scale circulations, further local analyses are required to understand this phenomenon fully.

Acknowledgements

Thanh-Hoa Pham-Thi is supported by the Tokyo Human Resources Fund for Diplomacy of the Tokyo Metropolitan Government, Japan. Thanh-Hoa Pham-Thi, Jun Matsumoto,

and Masato I. Nodzu are supported by the 2nd Research Announcement on the Earth Observations (JX-PSPC-513012) from the JAXA. We also thank the NCHMF, the VNMHA for providing the synoptic rainfall dataset used in this study. We appreciate two anonymous reviewers and editors whose constructive comments helped to improve the manuscript.

References

Bao X., Zhang F., Sun J., 2011. Diurnal variations of warm-season precipitation east of the Tibetan Plateau over China. Mon. Wea. Rev., 139, 2790-2810.

Battaglia A., Mroz K., Watters D., Ardhuin F., 2020. GPM-derived climatology of attenuation due to clouds and precipitation at Ka-band. IEEE T. Geosci., Remote., 58, 1812-1820.

Carbone R.E., Tuttle J.D., Ahijevych D.A., Trier S.B., 2002. Inferences of predictability associated with warm season precipitation episodes. J. Atmos. Sci., 59, 2033-2056.

Chen G., Sha W., Iwasaki T., 2009. Diurnal variation of precipitation over southeastern China: Spatial distribution and its seasonality. J. Geophys. Res., 114, D13103.

Chen G., Lan R., Zeng W., Pan H., Li W., 2018. Diurnal variations of rainfall in surface and satellite observations at the monsoon coast (South China). J. Climate, 31, 1703-1724.

Chen G., 2020. Diurnal cycle of the Asian summer monsoon: Air pump of the second kind. J. Climate, 33, 1747-1775.

Dai A., 2001. Global precipitation and thunderstorm frequencies. Part II: Diurnal variations. J. Climate, 14, 1112-1128.

Dinku T., Ceccato P., Grover-Kopec E., Lemma M., Connor S.J., Ropelewski C.F., 2007. Validation of satellite rainfall products over East Africa's complex topography. Int. J. Remote Sens., 28, 1503-1526.

Gao Y.C., Liu M.F., 2013. Evaluation of high-resolution satellite precipitation products using rain gauge observations over the Tibetan Plateau. Hydrol. Earth Syst. Sci., 17, 837-849.

Guo H., Chen S., Bao A., Hu J., Gebregiorgis A., Xue X., Zhang X., 2015. Inter-comparison of high-resolution satellite precipitation products over Central Asia. Remote Sensing, 7, 7181-7211.

Hastings D.A., Dunbar P.K., 1999. Global Land One-kilometer Base Elevation (GLOBE) digital elevation model, version 1.0. National Oceanic and Atmospheric Administration, National Geographysical Data Center, digital media. Available online at https://iridl.ldeo.columbia.edu/SOURCES/.NOAA/.NGDC/.GLOBE/topo/datafiles.html. Accessed 12 May 2021.

He H., Zhang F., 2010. Diurnal variations of warm-season precipitation over Northern China. Mon. Wea. Rev., 138, 1017-1025.

Hirose M., Nakamura K., 2005. Spatial and diurnal variation of precipitation systems over Asia observed by the TRMM Precipitation Radar. J. Geophys. Res., 110, D05106.

Huang H.-L., Wang C.-C., Chen G.T.-J., Carbone R.E., 2010. The role of diurnal solenoidal circulation on propagating rainfall episodes near the eastern Tibetan Plateau. Mon. Wea. Rev., 138, 2975-2989.

Huffman G.J., Bolvin D.T., Nelkin E.J., Wolff D.B., Adler R.F., Gu G., Hong Y., Bowman K.P., Stocker E.F., 2007. The TRMM Multisatellite Precipitation Analysis (TMPA): Quasi-Global, Multiyear, Combined-sensor precipitation estimates at fine scales. J. Hydrol., 8, 38-55.

Joyce R.J., Janowiak J.E., Arkin P.A., Xie P., 2004. CMORPH: A method that produces global precipitation estimates from passive microwave and infrared data at high spatial and temporal resolution. J. Hydrometeor., 5, 487-503.

Kubota T., Ushio T., Shige S., Kida S., Kachi M., Okamoto K., 2009. Verification of high-resolution satellite-based rainfall estimates around Japan using a gauge-calibrated ground-radar dataset. J. Meteor. Soc. Japan, 87A, 203-222.

Kummerow C., Simpson J., Thiele O., Barnes W., Chang A.T.C., Stocker E., Adler R.F., Hou A., Kakar R., Wentz F., Ashcroft P., Kozu T., Hong Y., Okamoto K., Iguchi T., Kuroiwa H., Im E., Haddad Z., Huffman G., Ferrier B., Olson W.S., Zipser E., Smith E.A., Wilheit T.T., North G., Krishnamurti T., Nakamura K., 2000. The status of the Tropical Rainfall Measuring Mission (TRMM) after two years in orbit. J. Appl. Meteor., 39, 1965-1982.

Lewis E., Fowler H.J., Alexander L., Dunn R., McClean F., Barbero R., Guerreiro S., Li X.F., Blenkinsop S., 2019. GSDR: a global sub-daily rainfall dataset. J. Climate, 32, 4715-4729.

Li J., Yu R., Zhou T., 2008. Seasonal variation of the diurnal cycle of rainfall in southern contiguous China. J. Climate, 21, 6036-6043.

Matsumoto J., 1997. Seasonal transition of summer rainy season over indochina and adjacent monsoon region. Adv. Atmos. Sci., 14, 231-245.

Mega T., Shige S., 2016. Improvements of Rain/No-Rain classification methods for microwave radiometer over coasts by dynamic surface-type classification. J. Atmos. Ocean. Tech., 33, 1257-1270.

Mega T., Ushio T., Takahiro M., Kubota T., Kachi M., Oki R., 2019. Gauge-adjusted global satellite mapping of precipitation. IEEE T. Geosci., Remote., 57, 1928-1935.

Minobe S., Park J.H., Virts K.S., 2020. Diurnal cycles of precipitation and lightning in the tropics observed by TRMM3G68, GSMaP, LIS, and WWLLN. J. Climate, 33, 4293-4313.

Nesbitt S.W., Zipser E.J., 2003. The diurnal cycle of rainfall and convective intensity according to three years of TRMM measurements. J. Climate, 16, 1456-1475.

Ngo-Duc T., Matsumoto J., Kamimera H., Bui H.-H., 2013. Monthly adjustment of Global Satellite Mapping of Precipitation (GSMaP) data over the VuGia-ThuBon river basin in Central Vietnam using an artificial neural network. Hydrol. Res. Lett., 7, 85-90.

Nguyen-Le D., Matsumoto J., Ngo-Duc T., 2014. Climatological onset date of summer monsoon in Vietnam. Int. J. Climatol., 34, 3237-3250.

Nguyen-Le D., Matsumoto J., Ngo-Duc T., 2015. Onset of the rainy seasons over the eastern Indochina Peninsula. J. Climate., 28, 5645-5666.

Nguyen-Le D., Matsumoto J., 2016. Delayed withdrawal of the autumn rainy season over central Vietnam in recent decades. Int. J. Climatol., 36, 3002-3019.

Nodzu M.I., Matsumoto J., Trinh-Tuan L., Ngo-Duc T., 2019. Precipitation estimation performance by Global Satellite Mapping and its dependence on wind over northern Vietnam. Prog. Earth Planet. Sci., 6, 58.

Ohsawa T., Ueda H., Hayashi T., Watanabe A., Matsumoto J., 2001. Diurnal variations of convective activity and rainfall in tropical Asia. Jour. Met. Soc. Japan. Ser. II, 79, 333-352.

Oki T., Musiake K., 1994. Seasonal change of the diurnal cycle of precipitation over Japan and Malaysia. J. Appl. Meteor., 33, 1445-1463.

Pfeifroth U., Trentmann J., Fink A.H., Ahrens B., 2016. Evaluating Satellite-Based Diurnal Cycles of Precipitation in the African Tropics. J. Appl. Meteor. Climatol., 55, 23-39.

Pham-Thi T.-H., Matsumoto J., 2021. Intercomparison of Global Satellite Mapping of Precipitation (GSMaP) using rain-gauge observations based on multiple temporal resolutions in Vietnam. Geog. Reps. Tokyo Metrop. Univ., 56, 33-44.

Shige, S., Kida, S., Ashiwake, H., Kubota, T., Aonashi, K., 2013. Improvement of TMI rain retrievals in mountainous areas. J. Appl. Meteor. Climatol. 52, 242-254.

Takahashi H.G., Fujinami H., Yasunari T., Matsumoto J., 2010. Diurnal rainfall pattern observed by Tropical Rainfall Measuring Mission Precipitation Radar (TRMM-PR) around the Indochina peninsula. J. Geophys. Res., 115, D07109.

Takahashi, H.G., 2013. Orographic low-level clouds of Southeast Asia during the cold surges of the winter monsoon. Atmos. Res., 131, 22-33.

Takahashi H.G., 2016. Seasonal and diurnal variations in rainfall characteristics over the Tropical Asian monsoon region using TRMM-PR data. SOLA, 12A, 22-27.

Trinh-Tuan L., Matsumoto J., Ngo-Duc T., Nodzu M.I., Inoue T., 2019. Evaluation of satellite precipitation products over Central Vietnam. Prog. Earth Planet. Sci., 6, 54.

Ushio T., Sasashige K., Kubota T., Shige S., Okamoto K., Aonashi K., Inoue T., Takahashi N., Iguchi T., Kachi M., Oki R., Morimoto T., Kawasaki Z.-I., 2009. A Kalman filter approach to the Global Satellite Mapping of Precipitation (GSMaP) from combined passive microwave and infrared radiometric data. Jour. Met. Soc. Japan, 87A, 137-151.

Wang B., 2002. Rainy season of the Asian-Pacific summer monsoon. J. Climate, 15, 386-398.

Watters D., Battaglia A., 2019. The summertime diurnal cycle of precipitation derived from IMERG. Remote Sensing, 11, 1781.

Xiao C., Yuan W., Yu R., 2018. Diurnal cycle of rainfall in amount, frequency, intensity, duration, and the seasonality over the UK. Int. J. Climatol., 38, 4967-4978.

Xu W., Zipser E.J., 2011. Diurnal variations of precipitation, deep convection, and lightning over and east of the eastern Tibetan Plateau. J. Climate, 24, 448-465.

Yokoi S., Matsumoto J., 2008. Collaborative effects of cold surge and tropical depression-type disturbance on heavy rainfall in Central Vietnam. Mon. Wea. Rev., 136, 3275-3287.

Yu R., Xu Y., Zhou T., Li J., 2007. Relation between rainfall duration and diurnal variation in the warm season precipitation over central eastern China. Geophys. Res. Lett., 34, L13703.

Yuan W., Yu R., Zhang M., Lin W., Chen H., Li J., 2012. Regimes of diurnal variation of summer rainfall over subtropical East Asia. J. Climate, 25, 3307-3320.